

# Antisense oligonucleotides with oxetane-constrained cytidine enhance heteroduplex stability, and elicit satisfactory RNase H response as well as showing improved resistance to both exo and endonucleases †

Pushpangadan, I. Pradeepkumar, Nariman V. Amirkhanov and Jyoti Chattopadhyaya \*

Department of Bioorganic Chemistry, Biomedical Center, University of Uppsala, Box 581, S-751 23 Uppsala, Sweden. E-mail: jyoti@boc.uu.se; Fax: +4618554495

Received 15th October 2002, Accepted 15th October 2002

First published as an Advance Article on the web 26th November 2002

Antisense oligonucleotides (AONs) with single and double oxetane **C** modifications [1',2'-oxetane constrained cytidine, 1-(1',3'-*O*-anhydro- $\beta$ -D-psicofuranosyl)cytosine] have been evaluated, in comparison with the corresponding **T**-modified AONs, for their antisense potentials by targeting to a 15mer complementary RNA. Although the **C** modified mixmer AONs show  $\sim 3$  °C drop per modification in melting temperature ( $T_m$ ) of their hybrid AON–RNA duplexes, they are found to be good substrates for RNase H, in comparison with the native AON–RNA duplex. An AON with double **C** modifications along with 3'-DPPZ (dipyridophenazine) conjugation shows the  $T_m$  of the hybrid duplexes as high as that of the native, and the RNase H activity as good as its unconjugated counterpart. A detailed Michaelis–Menten kinetic analysis of RNase H cleavage showed that the single and double **C** modified AON–RNA duplexes as well as double **C** modifications along with 3'-DPPZ have catalytic activities ( $k_{cat}$ ) close to the native. However, the RNase H binding affinity ( $1/K_m$ ) showed a slight decrease with increase in the number of modifications, which results in less effective enzyme activity ( $k_{cat}/K_m$ ) for **C** modified AON–RNA duplexes. All oxetane modified AON–RNA hybrids showed a correlation of  $T_m$  with the  $1/K_m$ ,  $V_{max}$ , or  $V_{max}/K_m$ . The **C** modified AONs (with 3'-DPPZ), as in the **T** counterpart, showed an enhanced tolerance towards the endonuclease and exonuclease degradation compared to the native (the oxetane-sugar and the DPPZ based AONs are non-toxic to K562 cell growth, ref. 18). Thus a balance has been found between exo and endonuclease stability *vis-a-vis* thermostability of the heteroduplex and the RNase H recruitment capability and cleavage with the oxetane-constrained cytidine incorporated AONs as potential antisense candidates with a fully phosphate backbone for further biological assessment.

## Introduction

Antisense Oligonucleotides (AONs) down-regulate gene expression (Fig. 1) by complexing with the target mRNA in two

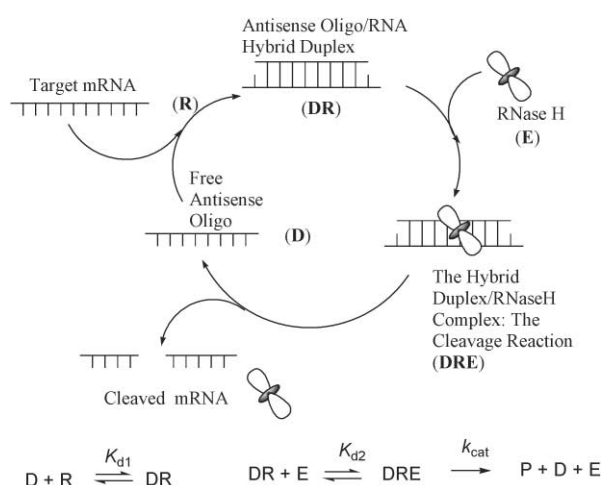


**Fig. 1** The catalytic RNase H promoted cleavage of the target mRNA through the formation of an antisense oligonucleotide–RNA hybrid duplex. The kinetic scheme of the RNase H hydrolysis is shown in the bottom part of the cartoon, where **D** is AON (antisense oligo); **R** is the target RNA;  $K_{d1}$  is the equilibrium constant of dissociation of the heteroduplex **DR**;  $K_{d2}$  is equilibrium constant of dissociation of the substrate–enzyme complex **DRE**.

† Electronic supplementary information (ESI) available: RNA cleavage kinetics. See <http://www.rsc.org/suppdata/ob/b2/b210163g/>

different ways:<sup>1</sup> (1) Translational arrest of the message by tight binding to the target mRNA (steric blocking of ribosomal machinery), which requires at least stoichiometric amounts of AON to the target. (2) The catalytic cleavage of the target mRNA in the AON–RNA hybrid by the activation of RNase H, which is a ubiquitous enzyme in all cells.<sup>2</sup> The latter strategy based on RNase H activation has intrinsic advantages over the steric blocking because it requires only a relatively small amount of AON, compared to the former, causing permanent destruction of the translated message with catalytic turnover, provided the AON has enough life time (stability) in cells.<sup>1</sup> The RNase H insensitive AONs employed so far for the translational arrest have relatively high melting temperature ( $T_m$ ), which may bind to other targets with one or two mismatches owing to poor discrimination. Hence, considerable attention has been directed in the design, synthesis and evaluation of AONs which are capable to recruit RNase H keeping the target affinity close to the unmodified duplex.<sup>2b</sup> The first generation AONs, the nucleolytically stable phosphorothioates, although working by utilizing the RNase H mechanism, its low binding affinity to the target RNA, less sequence specificity and strong affinity to heparin-binding proteins<sup>3</sup> (one to three order magnitude higher than the corresponding phosphodiester oligonucleotide) generate plenty of non-antisense effects, which in turn limit its therapeutic potential.<sup>3</sup> Chimeric oligonucleotides (gapmers) based on a phosphorothioate backbone (second generation AONs) with various 2'-*O*-alkyl modifications<sup>4,5</sup> at the 3'- and 5'-ends and 4 to 6 unmodified nucleotides in the middle, although showing enhanced binding affinity, fail to keep the RNase H cleavage as good as the native phosphorothioate or phosphodiester counterparts.<sup>5</sup> An increment of gapsize has

been shown to increase the RNase H activity;<sup>6</sup> however, it has the disadvantage that these gapmers are more exposed to endonuclease degradations.<sup>7</sup> Chimeric AONs based on methylphosphonates<sup>8</sup> and AONs based on boranophosphates<sup>9</sup> show enhanced RNase H activity but poor affinity to the RNA target.

The search for an ideal chemistry (without changing the phosphodiester backbone) which is capable of giving *bona fide* antisense action has intensified in the past decade: oligos incorporating conformationally (3'-*endo*) constrained nucleosides<sup>10,11</sup> show enhanced stability of the resulting AON–RNA hybrid duplex. The enhanced stability of conformationally constrained AONs is attributed to the formation of a rigid A type AON–RNA duplex (reminiscent of an RNA–RNA type duplex) which accounts for the loss of RNase H recruiting capability.<sup>2b,4</sup>

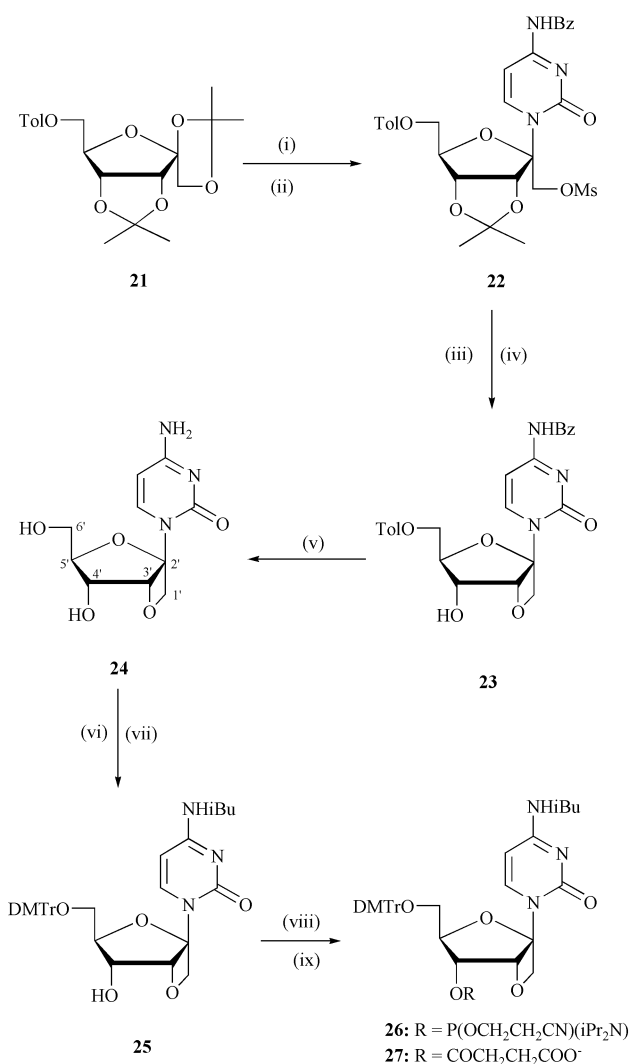
Within the family of conformationally constrained nucleotides, we have recently<sup>12</sup> reported the RNase H recruiting capabilities of north-east constrained *oxetane thymidine*, **T** [1-(1',3'-*O*-anhydro- $\beta$ -D-psicofuranosyl)thymine, Fig. 2] modified mixmer AONs where we have shown that, although  $T_m$  drops by  $\sim 6$  °C per modification, the RNase H cleavage of the target RNA remain intact or increased compared to the wild type heteroduplex, under enzyme saturation conditions<sup>12c</sup> (enzyme is completely saturated by substrate, AON–RNA duplex). Although the **T** modification did not alter the global helical structure of the modified AON–RNA duplex in comparison with the wild type duplex<sup>12</sup> (as revealed by CD spectra), the target RNA strand in the AON–RNA duplex was resistant to RNase H promoted cleavage, up to 5 nucleotides towards the 3'-end from the site opposite to the **T** introduction, because of subtle alteration of the microenvironment as a result of **T** incorporation.<sup>12</sup>

A detailed Michaelis–Menten type kinetic analysis of triple **T** modified AON–RNA hybrid has also been carried out<sup>13</sup> to understand the mechanism of RNase H recruitment, substrate recognition, specificity and cleavage *vis-à-vis* conformational preorganization of the hybrid duplex. It has emerged that the  $V_{max}$  and the  $K_m$  were respectively  $\sim 2$  and  $\sim 10$  times more for the triple **T** oxetane modified AON–RNA duplex than those for the native counterpart, which shows the increase in the catalytic activity of the oxetane modified AON–RNA duplex almost 2 fold owing to the decreased affinity of the substrate toward the enzyme.<sup>13</sup>

The single, double and triple **T** oxetane modified AONs have been shown to have 3 to 5 fold protection<sup>12c</sup> towards endonuclease which augments its antisense potential through the RNase H assisted pathway. We have also shown that the  $T_m$  loss, owing to oxetane modifications, can be regained (+8 °C) by the introduction of a DPPZ<sup>14</sup> (dipyridophenazine) moiety at the 3'-end of the AON without sacrificing RNase H eliciting and cleavage power.<sup>12c</sup>

The 3'-DPPZ moiety also renders the AONs stable towards 3'-exonucleases.<sup>12c,14b</sup> Interestingly, the tethering of DPPZ in a native 9mer AON has been shown<sup>15</sup> to increase the effective enzyme activity ( $V_{max}/K_m$ ) of the RNase H by six fold compared to the native 9mer AON and two fold compared to the high hydrophobic 3'-tethers like cholesterol<sup>15,16a–e</sup> and cholic acid<sup>17</sup> because of the high binding affinity ( $1/K_m$ ) of DPPZ modified AON–RNA duplex to the enzyme.<sup>15</sup> It has also been found that the introduction of DPPZ moiety to oxetane modified mixmer AONs to be non-toxic in various cell culture assays.<sup>18</sup>

In view of the novel antisense properties of oxetane modified AONs containing **T** modifications, we here report the synthesis of oxetane **C** [1-(1',3'-*O*-anhydro- $\beta$ -D-psicofuranosyl)cytosine, (**24**) in Scheme 1] modified AONs (**5**, **6**, **13**, Fig. 2) and their 3'-DPPZ (**9**) and cholesterol **11** conjugated AONs. We also report the hybridization properties of these AONs to the target RNA **14**, as well as their exo and endonuclease resistance properties along with a detailed kinetic analysis of RNase H



**Scheme 1** Reagents and conditions: (i) persilylated N<sup>4</sup>-Bz-cytosine, acetonitrile, TMSOTf, 0 °C to rt, 18 h; (ii) MsCl, pyridine, 4 °C, 12 h; (iii) 90% TFA–water, rt, 20 min; (iv) NaH, DMF, 4 °C, 9 h; (v) methanolic NH<sub>3</sub>, rt, 48 h; (vi) TMSCl, pyridine, rt, 30 min followed by *i*BuCl, rt, 3 h; (vii) DMTrCl, pyridine, rt, 12 h; (viii) (2-cyanoethoxy)bis(*N,N*-diisopropylamino)phosphine, *N,N*-diisopropylammonium tetrazolide, DCM, 12 h for **26**; (ix) succinic anhydride, DMAP, DCM, 4 h, rt, for **27**. Abbreviations: Tol = 4-methylbenzoyl, Bz = benzoyl, TMSOTf = trimethylsilyl trifluoromethane sulfonate, rt = room temperature, Ms = methanesulfonyl, DMTr = dimethoxytrityl, Et = ethyl, TFA = trifluoroacetic acid, *i*Bu = isobutyl, DCM = dichloromethane, TMS = trimethylsilyl, DMAP = dimethylamino-pyridine.

cleavage of single and double **C** modified AON–RNA hybrid duplexes in comparison with the corresponding **T** modified AON (**2–4**)–RNA (**14**) and the native 15mer AON (**1**)–RNA (**14**) duplexes.

## Results

### (1) Endonuclease (DNase I) stability

When tested for endonuclease stability using DNase I, the single **C** modified AON **5** showed more than 3 fold protection (60% left after 1 h), while the double **C** modified AON **6** gave 4–5 fold protection (93% left), whereas two **C** modifications with 3'-terminal DPPZ showed also 4–5 fold protection (98% left) compared with native AON **1** (24% left after 1 h) (Fig. 3). The stability achieved by double **C** modifications was comparable to, or better than, that of the phosphorothioate AON **12** (88% of AON left after 1 h incubation) (Fig. 3). The similar behaviour of endonuclease tolerance has been reported for various **T** modified AONs.<sup>12c</sup>

Native 15mer (PO)	AON (1)	3'-d(CTTC TTTTTTACTTC)-5'	$T_m = 44\text{ }^\circ\text{C}$ , $\Delta T_m = 0\text{ }^\circ\text{C}$
15-1 <u>T</u>	AON (2)	3'-d(CTTC TTTTTT <u>T</u> ACTTC)-5'	$T_m = 39\text{ }^\circ\text{C}$ , $\Delta T_m = -6\text{ }^\circ\text{C}$
15-2 <u>T</u>	AON (3)	3'-d(CT <u>T</u> CTTTTT <u>T</u> ACTTC)-5'	$T_m = 33\text{ }^\circ\text{C}$ , $\Delta T_m = -11\text{ }^\circ\text{C}$
15-3 <u>T</u>	AON (4)	3'-d(CT <u>T</u> CTTTTT <u>T</u> TTACT <u>T</u> C)-5'	$T_m = 26\text{ }^\circ\text{C}$ , $\Delta T_m = -18\text{ }^\circ\text{C}$
15-1 <u>C</u>	AON (5)	3'-d(CTT <u>C</u> TTTTTTACTTC)-5'	$T_m = 41\text{ }^\circ\text{C}$ , $\Delta T_m = -3\text{ }^\circ\text{C}$
15-2 <u>C</u>	AON (6)	3'-d(CTT <u>C</u> TTTTTTA <u>C</u> TTTC)-5'	$T_m = 38\text{ }^\circ\text{C}$ , $\Delta T_m = -6\text{ }^\circ\text{C}$
15-DPPZ	AON (7)	DPPZ-p-3'-d(CTTC TTTTTTACTTC)-5'	$T_m = 49\text{ }^\circ\text{C}$ , $\Delta T_m = +5\text{ }^\circ\text{C}$
15-3 <u>T</u> -DPPZ	AON (8)	DPPZ-p-3'-d(CT <u>T</u> CTTTTT <u>T</u> TTACT <u>T</u> C)-5'	$T_m = 34\text{ }^\circ\text{C}$ , $\Delta T_m = -10\text{ }^\circ\text{C}$
15-2 <u>C</u> -DPPZ	AON (9)	DPPZ-p-3'-d(CTT <u>C</u> TTTTTTA <u>C</u> TTTC)-5'	$T_m = 44\text{ }^\circ\text{C}$ , $\Delta T_m = 0\text{ }^\circ\text{C}$
15-3 <u>T</u> -Cholest	AON (10)	Cholest-p-3'-d(CT <u>T</u> CTTTTT <u>T</u> TTACT <u>T</u> C)-5'	$T_m = 29\text{ }^\circ\text{C}$ , $\Delta T_m = -15\text{ }^\circ\text{C}$
15-2 <u>C</u> -Cholest	AON (11)	Cholest-p-3'-d(CTT <u>C</u> TTTTTTA <u>C</u> TTTC)-5'	$T_m = 40\text{ }^\circ\text{C}$ , $\Delta T_m = -4\text{ }^\circ\text{C}$
Native 15mer (PS)	AON (12)	3'-d(CTTC TTTTTTACTTC)-5'	$T_m = 31\text{ }^\circ\text{C}$ , $\Delta T_m = -13\text{ }^\circ\text{C}$
15-3'- <u>C</u> modified	AON (13)	3'-d( <u>C</u> TTC TTTTTTACTTC)-5	
Target 15mer RNA	RNA (14)	5'-r(GAAGAAAAAUGAAG)-3'	
Native 9mer (PO)	AON (15)	3'-d(TCCAAACAT)-5'	$T_m = 20\text{ }^\circ\text{C}$ , $\Delta T_m = 0\text{ }^\circ\text{C}$
9-Chol	AON (16)	Chol-p-3'-d(TCCAAACAT)-5'	$T_m = 25\text{ }^\circ\text{C}$ , $\Delta T_m = +5\text{ }^\circ\text{C}$
9-Chol(Ac) <sub>3</sub>	AON (17)	Chol(Ac) <sub>3</sub> -p-3'-d(TCCAAACAT)-5'	$T_m = 24\text{ }^\circ\text{C}$ , $\Delta T_m = +4\text{ }^\circ\text{C}$
9-Cholest	AON (18)	Cholest-p-3'-d(TCCAAACAT)-5'	$T_m = 25\text{ }^\circ\text{C}$ , $\Delta T_m = +5\text{ }^\circ\text{C}$
9-DPPZ	AON (19)	DPPZ-p-3'-d(TCCAAACAT)-5'	$T_m = 31\text{ }^\circ\text{C}$ , $\Delta T_m = +11\text{ }^\circ\text{C}$
Target 17mer RNA (for 9mer AONs)	AON (20)	5'-r(ACUCAUGUUUGGACUCU)-3'	

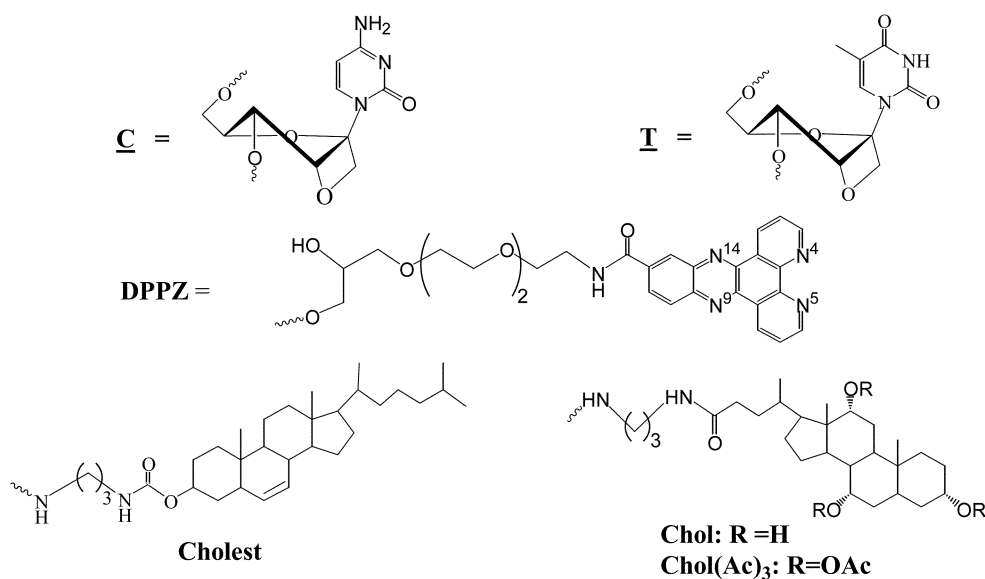


**Fig. 2** Sequences of various AONs and their target RNAs. The melting temperature ( $T_m$ ) and the difference in  $T_m$  ( $\Delta T_m$ ) with respect to the native phosphodiester AON 1 for 15mer AONs or AON 15 for 9mer AONs are also shown.

## (2) 3'-Exonuclease stability

We have subsequently examined the effect of 3'-exonuclease (snake venom phosphodiesterase, SVPDE) on C modification. For this, we have incorporated one C modification at the 3' end of AON 13. After 15 min, the native AON 1 with the phosphodiester backbone was found to be completely hydrolysed by the enzyme, whereas 60% of 3' C modified AON was intact after 1 h (Fig. 4). On the other hand, ca. 20% of interior double C modified AON 6 was left undigested by SVPDE after 1 h. (Fig. 4). As reported earlier, complete exonuclease resistance was achieved with DPPZ moiety at the 3'-end (97% of AON

9 left after 1 h of incubation), which was comparable to that of PS AON (96% of AON left after 1 h of incubation) (Fig. 4).

## (3) Human serum stability

The stability of AONs was also checked in human serum, where the major degrading enzymes present are 3'-exonucleases.<sup>7</sup> All DPPZ modified AONs (7–9) (62–68 % AON left after 1 h) showed comparable stabilities to that of PS AON (63% of AON left after 1 h) (Fig. 5), whereas the native AON was fully digested under identical conditions in 15 min.

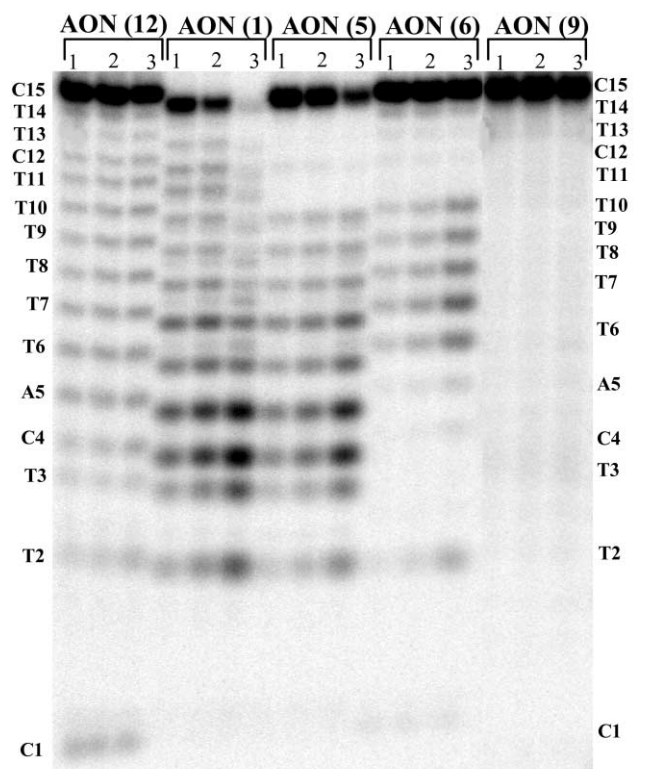


**Fig. 3** PAGE analysis of the DNase I degradation of AON 1, 5, 6, 9 and 12. Lanes 1 to 3 represent the time points after 30 min., 1 h and 3 h of reaction. The % of AON left after 1 h of incubation: 24% of AON 1, 88% of AON 12, 60% of AON 5, 93% of AON 6 and 98% of AON 9. Note a comparison of relative cleavage after 3 h that AON 9 shows even more stability to endonuclease (94%) than phosphorothioate AON 12 (82%).

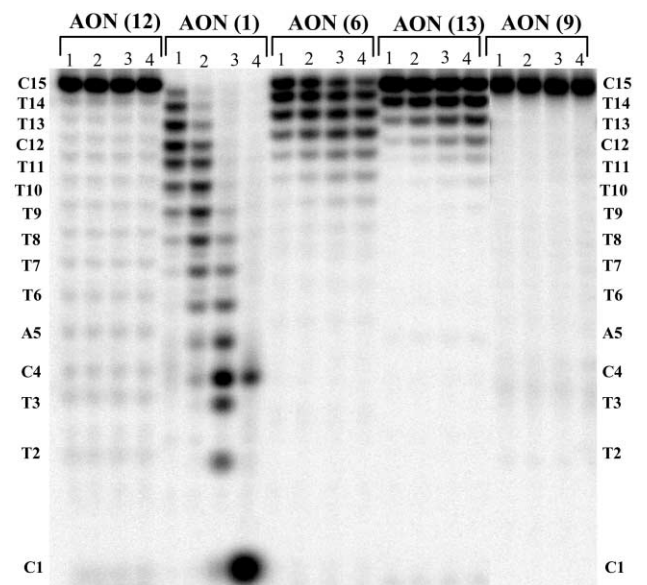


**Fig. 4** PAGE analysis of the snake venom phosphodiesterase (SVPDE) degradation of AONs 1, 6, 9, 12 and 13. Lanes 1 to 4 represent the time points after 15 min, 30 min, 1 h and 3 h of reaction. The % of AON left after 1 h of incubation with enzyme: 0% of AON 1, 95% of AON 12, 20% of AON 6, 60% of AON 13 and 97% of AON 9.

#### (4) Binding affinity of the oxetane-modified antisense oligos to the target RNA

The incorporation of single C modification as in AON 5–RNA 14 causes 3 °C drop in  $T_m$  ( $T_m = 41$  °C) with respect to the unmodified AON 1–RNA 14 hybrid duplex ( $T_m = 44$  °C, Fig. 1). The incorporation of two C modifications caused 6 °C drop in  $T_m$  of the AON 6–RNA duplex. This should be

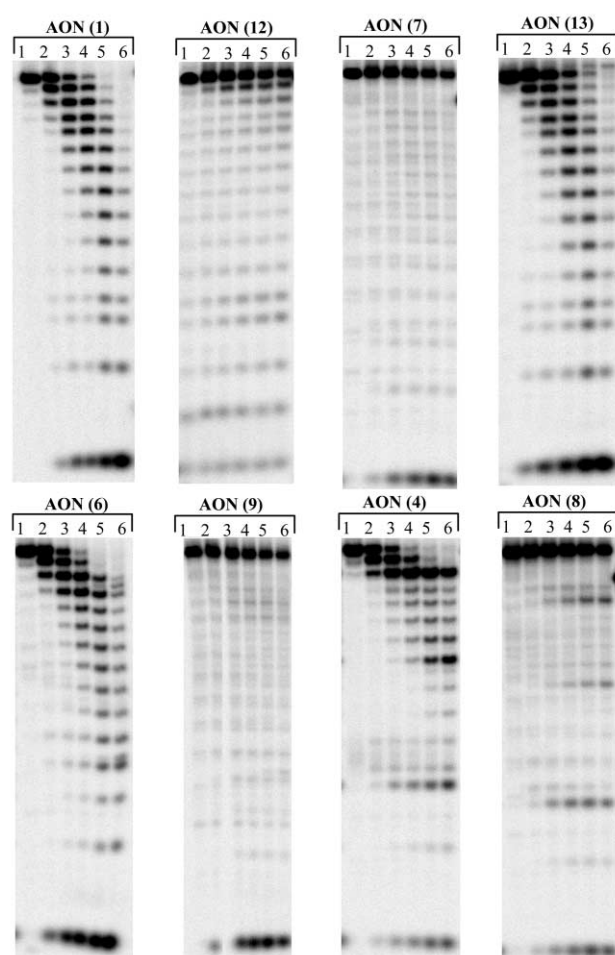


**Fig. 5** PAGE analysis of the degradation of AON 1, 12, 7, 13, 6, 9, 4 and 8 in human serum. Lanes 1 to 6 represents the time points after 0, 5, 15 and 30 min, 1 h and 2 h of reaction. The % of AON left after 1 h of incubation: 0% of AON 1, 63% of AON 12, 62% of AON 7, 0% of AON 13, 0% of AON 6, 64% of AON 9, 0% of AON 4 and 68% of AON 8.

compared with the corresponding T modification<sup>12</sup>, which leads to a ~6 °C drop in  $T_m$  per modification. However, the loss in  $T_m$  owing to two C modifications, for example, is fully restored to the level of native hybrid duplex by the introduction of a dipyridophenazine (DPPZ) moiety at the 3' end ( $T_m = 44$  °C), as in AON 9. It has also been found that the introduction of DPPZ moiety to oxetane T and oxetane C modified mixmer AONs to be non-toxic in various cell culture assays.<sup>18</sup> Conjugation of the cholesterol<sup>15,16</sup> moiety at the 3'-end of the T and C modified oxetane also increases  $T_m$  of the hybrid AON–RNA duplexes in comparison to their unconjugated counterparts (Fig. 2). However, increase in  $T_m$  in the case of the cholesterol conjugated AONs (10 and 11) ( $\Delta T_m = \sim 2.5$  °C) is less than in the case of DPPZ conjugated ones (8 and 9) ( $\Delta T_m = 5$  to 8 °C). Thus incorporation of C modifications has clear advantages over T modifications in the construction of AONs as far as the target RNA affinity is concerned.

#### (5) RNase H cleavage pattern of complementary RNA in heteroduplexes containing C oxetane modified AONs and their DPPZ and cholesterol conjugates

The single C or double C modified AON (5 or 6)–RNA (14) hybrids were found to be as good a substrate for RNase H as found for the T modified AONs<sup>12</sup> (Fig. 6, see also Fig. S1–S3, S4–S14 in supplementary information). In all the C modified hybrid duplexes including DPPZ and cholesterol conjugates, 5 nucleotides towards the 3'-end from the site opposite to the C introduction were found to be insensitive towards RNase H

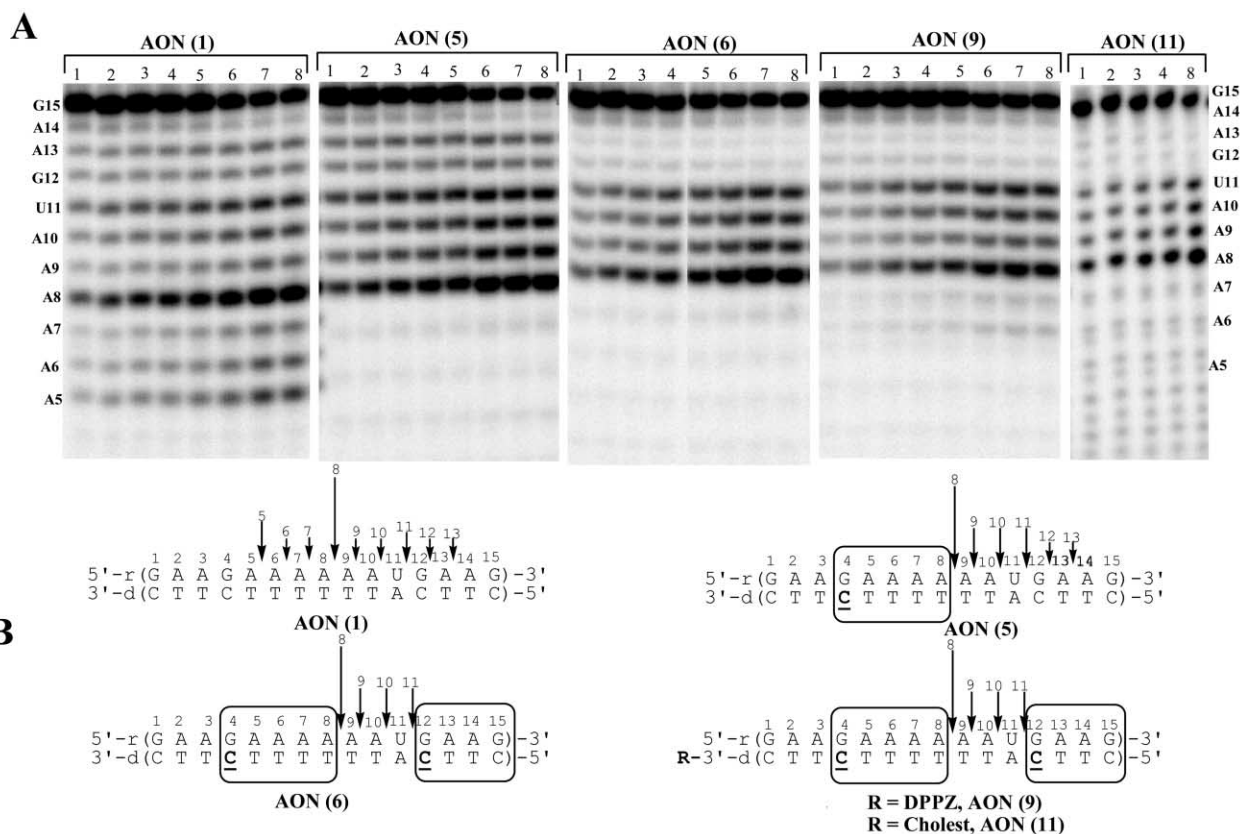


**Fig. 6 (A):** Autoradiograms of 20% denaturing PAGE, showing the cleavage kinetics of 5'-<sup>32</sup>P-labelled target RNA **14** by RNase H1 in the native AON **1**-RNA **14** and oxetane **C** modified AON (**5,6,9,11**)-RNA **14** hybrid duplexes. Lanes 1 to 8 represents the aliquots of the digest taken after 2, 3, 4, 5, 6, 20, 40 and 60 min respectively. Conditions of cleavage reaction: RNA (0.04  $\mu$ M) and AONs (5  $\mu$ M) in buffer, containing 20 mM Tris-HCl (pH 8.0), 20 mM KCl, 10 mM MgCl<sub>2</sub> and 0.1 mM DTT at 21 °C, 0.06 U of RNase H for AON **1, 5, 6, 9** and 0.12 U of RNase H for AON **11**. Total reaction volume is 30  $\mu$ l. The % of RNA left after 1 h: 38% of AON **1**, 36% of AON **5**, 54% of AON **6** 56% of AON **9** and 32% of AON **11**. **(B):** RNase H cleavage pattern of hybrid duplexes. The vertical arrows show the RNA cleavage sites and relative length of an arrow shows the relative extent of cleavage at that site.

promoted cleavage (Fig. 6, see also Fig. S1-S3, S15-S23), presumably owing to adoption of a local pseudo RNA-RNA type conformational character.<sup>12</sup> This 5-nucleotide footprint generated owing to RNase H resistance to cleavage reaction is identical to what has been earlier found for **T** modified AONs<sup>12</sup> (see also Fig. S4-S14). Conjugation of the DPPZ to triple **T** oxetane modified AON **8** results in an additional cleavage site compared to the unconjugated counterpart AON<sup>12c</sup> **4** (see also Figs S15-S23). No such additional cleavage site was found in the case of the DPPZ conjugated double **C** modified AON **9** compared to the unconjugated counterpart AON **6** (Fig. 6, see also Fig. S1-3). Conjugation of cholesterol moiety at the 3'-end of the **T** or **C** modified oxetane does not change RNA cleavage sites (Fig. 6, see also Fig. S15-23).

#### (6) Michaelis-Menten kinetics of **C** modified AONs and their DPPZ and cholesterol conjugates and its comparison with the **T** modified and native AONs

To understand the substrate specificity ( $K_m$ ,  $V_{max}$  and  $k_{cat}$ ) of RNA cleavage by RNase H in **C** modified AON-RNA hybrids, a detailed kinetic analysis of RNase H promoted cleavage of the RNA target in modified hybrid duplexes has been carried out, and subsequently compared with **T** modified AONs **2-4** and the native AON **1** (Fig. 6 and see also Figs S1-23). The initial velocities ( $v_0$ ) were calculated at different RNA concentration (at least in five different RNA concentrations, ([ $S_0$ ])), ranging from 0.008 to 3  $\mu$ M at 5  $\mu$ M AON under RNA **14** saturation conditions by AONs.<sup>13,15</sup>

The plot of  $v_0$  as a function of [ $S_0$ ] (Fig. 7) (materials and methods section) yielded the Michaelis-Menten parameters,<sup>19</sup>  $K_m$ ,  $V_{max}$  and  $k_{cat}$  (Table 1).

These data showed that the single and double **C** modified

AON (**5** and **6**)-RNA **14** duplexes have enzyme catalytic activity ( $V_{max}$  or  $k_{cat}$ ) close to the native AON **1**-RNA **14** duplexes (Table 1, Fig. 8A). However, the enzyme binding affinity ( $1/K_m$ ) showed a slight decrease with increase in number of modifications, which results in less effective enzyme activity ( $k_{cat}/K_m$ ) for **C** modified AON-RNA duplexes (Table 1, Figs. 8B and 8C). On the other hand, the kinetic data for **T** modified AON (**2-4**)-RNA **14** duplexes showed that the enzyme catalytic activity ( $V_{max}$ ) increases, whereas the binding affinity ( $1/K_m$ ) decreases with the increase in the number of **T** modifications, which gives less effective enzyme activity ( $k_{cat}/K_m$ ) compared to the native counterpart (Table 1, Fig. 8).

The introduction of a DPPZ moiety to the 3'-end of the double **C** modified AON (**9**) does not change the catalytic activity ( $V_{max}$ ) of the enzyme in comparison with the native AON **1** (Table 1, Fig. 8A). It decreases the  $1/K_m$  and  $k_{cat}/K_m$  in comparison with the native AON (**1**) (Table 1 and Fig. 8B, C). The introduction of a DPPZ moiety to the 3'-end of the triple **T** modified AONs **8** slightly decreases  $V_{max}$  value and the  $1/K_m$  of the enzyme, yielding a two fold lower  $k_{cat}/K_m$  value in comparison with the native counterpart (Table 1 and Figs. 8A-C). In contrast to DPPZ conjugated AONs, conjugation of a cholesterol residue to the AONs (**10** and **11**) increases the  $V_{max}$  values; however, the large drop in  $1/K_m$  results in the reduction of  $k_{cat}/K_m$  in comparison with the native AON **1**-RNA duplex (Table 1, Fig. 8).

#### (7) Correlation of Michaelis-Menten parameters with the thermostability of the heteroduplexes.

With the exception of the 3'-conjugated counterparts, all **C** and **T** modified AON-RNA hybrids have shown a linear correlation of the  $T_m$  of the hybrid duplexes with [ $\log(1/K_m)$ ], [ $\log(V_{max})$ ],

**Table 1** Kinetic characteristics<sup>a</sup> of RNA cleavage by RNase H in the AON (1–11)–RNA 14 hybrid duplexes

AONs	$T_m/^\circ\text{C}$	$V_{\max}/10^{-2} \mu\text{M min}^{-1}$	$K_m/10^{-2} \mu\text{M}$	$k_{\text{cat}}/\text{min}^{-1}$	$(V_{\max}/K_m)/\text{min}^{-1}$	$(k_{\text{cat}}/K_m)/\mu\text{M}^{-1} \text{min}^{-1}$	Relative ( $k_{\text{cat}}/K_m$ )
Native 15mer (1)	44	$1.9 \pm 0.3$	$5.7 \pm 1.1$	$84.4 \pm 11.5$	0.34	1476.9	1
<b>T-Oxetane modified AONs</b>							
15-1T (2)	39	$2.0 \pm 0.1$	$8.3 \pm 2.2$	$90.0 \pm 5.3$	0.25	1083.8	0.73
15-2T (3)	33	$2.4 \pm 0.1$	$11.2 \pm 1.7$	$104.9 \pm 4.0$	0.21	934.5	0.63
15-3T (4)	26	$3.4 \pm 0.3$	$40 \pm 2.9$	$165.8 \pm 11.2$	0.10	446.3	0.30
<b>C-Oxetane modified AONs</b>							
15-1C (5)	41	$2.0 \pm 0.1$	$6.4 \pm 0.9$	$88.6 \pm 3.5$	0.31	1376.3	0.93
15-2C (6)	38	$1.8 \pm 0.1$	$9.6 \pm 1.9$	$79.8 \pm 4.9$	0.19	828.8	0.56
<b>3'-DPPZ conjugated AONs</b>							
15-DPPZ (7)	49	$0.73 \pm 0.06$	$1.5 \pm 0.6$	$32.2 \pm 2.6$	0.50	2220	1.50
15-3T-DPPZ (8)	34	$1.4 \pm 0.2$	$10.4 \pm 3.7$	$62.2 \pm 7.1$	0.14	597.8	0.40
15-2C-DPPZ (9)	44	$1.9 \pm 0.1$	$12.6 \pm 2.1$	$81.6 \pm 4.4$	0.15	650.0	0.44
<b>3'-Cholesterol conjugated AONs</b>							
15-3T-Cholest (10)	29	$5.1 \pm 0.4$	$66.3 \pm 9.0$	$225.8 \pm 15.9$	0.08	340.7	0.23
15-2C-Cholest (11)	40	$3.5 \pm 0.3$	$30.9 \pm 6.6$	$153.5 \pm 13.2$	0.11	496.8	0.34

<sup>a</sup>  $V_{\max} = k_{\text{cat}} \times E_0$  ( $E_0 = 0.06 \text{ U per } 30 \mu\text{l} = 2 \times 10^{-3} \text{ U } \mu\text{l}^{-1} = 2.26757 \times 10^{-4} \mu\text{M}$ ), specific activity = 420000 U/mg or  $2.38 \times 10^{-6} \text{ mg U}^{-1} = 1.13386 \times 10^{-13}$  moles per unit, MW = 21 000 g mol<sup>-1</sup>.

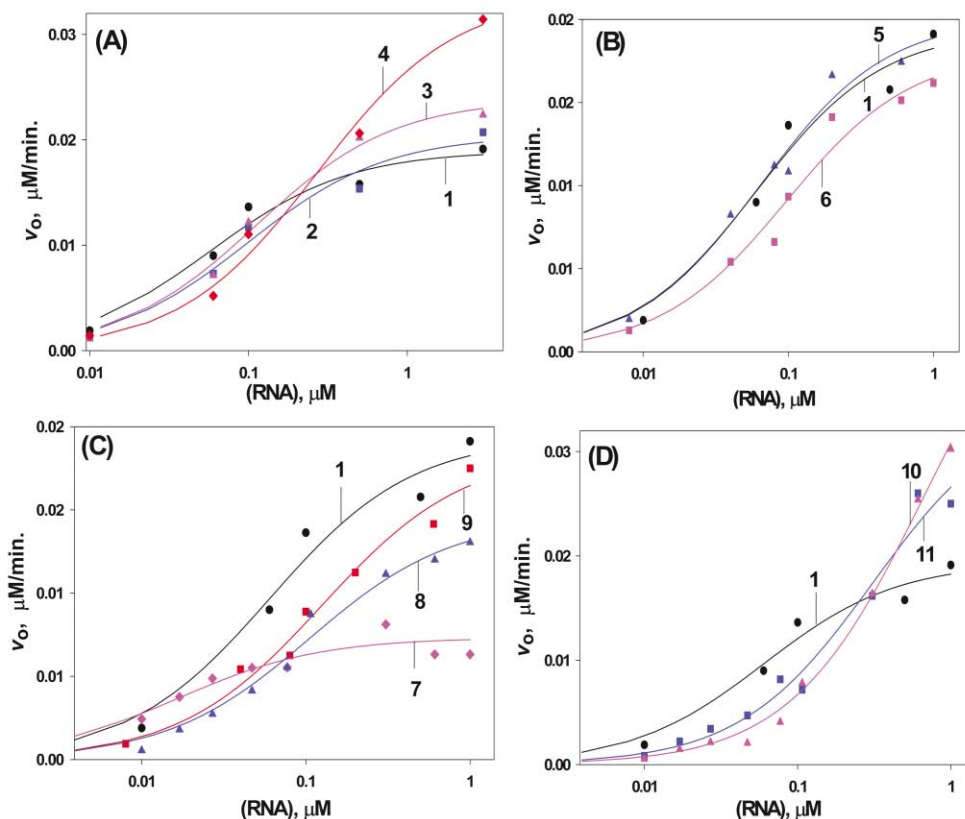


**Fig. 7** Initial velocity of the hydrolysis of the 15mer target RNA 14 in the AON (1–11)–RNA hybrids by RNase H as a function of the RNA concentration (logarithmic scale). Curves 1–11 correspond to the hybrid duplex formed by AONs 1–11 respectively. **A:** for unconjugated **T**-oxetane modified AONs 2–4. **B:** for unconjugated **C**-oxetane modified AONs 5 & 6. **C:** for DPPZ conjugated AONs 7–9. **D:** for cholesterol conjugated AONs 10, 11. Conditions of cleavage reaction: AONs (5 μM) and RNA 14 in buffer, containing 60 mM Tris-HCl (pH 7.5), 60 mM KCl, 10 mM MgCl<sub>2</sub> and 1 mM DTT at 21 °C, 0.06 U of RNase H. Total reaction volume is 30 μl.

or  $[\log(V_{\max}/K_m)]$  (Fig. 9). The enzyme binding affinity (Fig. 9B) and effective enzyme activity (Fig. 9C) increase with increase of  $T_m$ , however, the catalytic activity (Fig. 9A) was found to decrease with rise in thermostability of the hybrid duplexes.

### (8) Synthesis of oxetane **C** building blocks

1-(1',3'-*O*-Anhydro-β-D-psicofuranosyl)cytosine (**24**) in Scheme 1 was prepared from the sugar, 6'-*O*-toluoyl-1,2,3,4-di-

*O*-isopropylidene-β-D-psicofuranose<sup>12b</sup> (**21**) [Scheme 1]. Compound **21** was coupled with *N*,*O*-bis(trimethylsilyl)-*N*<sup>4</sup>-benzoylcytosine in the presence of TMSOTf as Lewis acid and acetonitrile as solvent to furnish an inseparable anomeric mixture of the protected psiconucleosides, which on mesylation gave **22** in 66% yield. Removal of the isopropylidene group from **22** using 90% CF<sub>3</sub>COOH in water at room temperature and subsequent cyclization with NaH in DMF gave **23** in moderate yield (49%). Detoluoylation of **23** furnished the desired

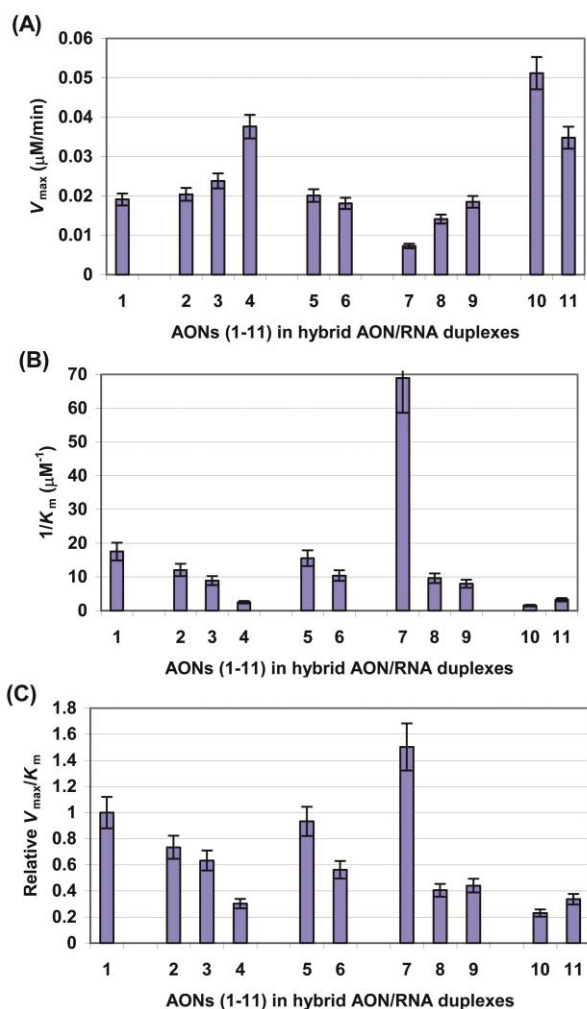


**Fig. 8** Bar graphs showing the  $V_{max}$  (A),  $1/K_m$  (B) and relative  $V_{max}/K_m$  (C) values for the RNase H promoted RNA hydrolysis in AON–RNA hybrid duplexes for native 15mer AON **1**, **T** and **C** oxetane modified AONs **2–6**, and their DPPZ and cholesterol conjugates **7–11**.

bicyclic nucleoside **24** (96%) and its  $\beta$  configuration at anomeric carbon was confirmed by NOE measurements (Experimental section). The nucleoside was converted into the corresponding phosphoramidite building block **26** (93%) via *N*<sup>4</sup>-isobutyryl-6'-*O*-(4,4'-dimethoxytrityl) protected derivative **25** for incorporation of **C** residues in the AONs (**5**, **6** and **9**) and the 4'-succinate **27** for the preparation of CPG solid support, which was used for the synthesis of AON **13**.

## Discussion

Several attempts have been made to engineer nuclease resistant antisense oligonucleotides, which both show high thermodynamic stability when bound to the complementary RNA, and are capable of recruiting RNase H as well as the native AON.<sup>2b,4,10,11</sup> Many of the conformationally constrained nucleotides in fact have been shown to enhance the stability of the modified AON–RNA heteroduplex, but failed to show any RNase H recruiting capability.<sup>2b,4,11</sup> It has emerged that (a) the optimal minor groove width (close to A type duplex,<sup>2b</sup> 8.9–10.8 Å), (b) the flexibility of the AON–RNA duplex, as well as (c) minimal stereochemical interference by the antisense strand in the minor groove (both structural, chemical as well as hydration points of view) of the heteroduplex–enzyme complex dictate the optimal RNase H activity.<sup>2b</sup> The intrinsic flexibility of the hybrid duplex enables it to form a complex with RNase H, resulting in a more stabilized structure, which allows the reactive amino acid residues at the active site of RNase H to stereochemically position themselves at the minor groove of the

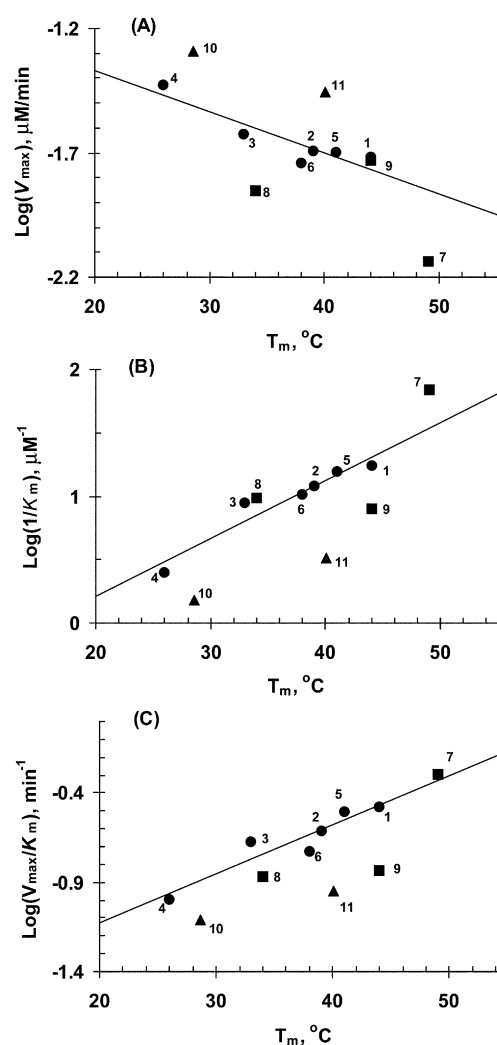


**Fig. 9** The plot of catalytic activity [ $\text{log}(V_{max})$ ] (A), binding affinity [ $\text{log}(1/K_m)$ ] (B) and effective activity [ $\text{log}(V_{max}/K_m)$ ] (C) of RNase H versus thermostability ( $T_m$ ) of the **C** and **T** modified AON–RNA duplexes and their DPPZ and cholesterol conjugates. Linear correlation was found for all unconjugated AONs (**1–6**)–RNA duplexes, except for the DPPZ ( $\blacksquare$ ) and cholesterol ( $\blacktriangle$ ) conjugates **7–11**. Note, those AONs (**7–11**) marked with ( $\blacksquare$ ) and ( $\blacktriangle$ ) are not included in the correlation equation. Correlation coefficients ( $R^2$ ) for the plots are: 0.92 for (A), 0.82 for (B) and 0.88 for (C).

duplex for the cleavage reaction to take place. Most of the north-constrained nucleosides were not able to fulfill these requirements.<sup>2,4,11b</sup> This was clearly evident with locked nucleic acids (LNA),<sup>10e,b,11b</sup> which showed high affinity to target RNA, but the mixer of LNA–RNA heteroduplexes failed to elicit any RNase H activity.<sup>20,21</sup> On the other hand, if in a gapmer the deoxynucleotide gaps between flanking LNAs are increased (6–10 native deoxynucleotide gaps), the flexibility in the deoxynucleotide gap is enhanced, which elicits the RNase H activity.<sup>6</sup> We have earlier observed<sup>12</sup> such footprints in the RNA cleavage pattern by RNase H owing to the altered AON–RNA conformation in the conformationally constrained oxetane-modified heteroduplex. It should be noted that the fifth internucleoside phosphate residue from the 5'-end of the complementary RNA strand is cleaved by RNase H in the case with our oxetane based AONs, whereas it is at the seventh phosphate where the enzymatic cleavage takes place with LNA incorporated AONs.<sup>6</sup>

The oxetane **C** based AONs have more affinity to the target RNA than oxetane **T** modified AONs (Fig. 2). AONs with two **C** modifications in conjunction with a tethered 3'-DPPZ group have a phosphodiester (PO) backbone, as in AON **9**, which has an almost identical hybrid AON **9**–RNA **14** stability to that of

the native duplex AON 1–RNA 14; both have  $T_m$ s of 44 °C (Fig. 2), thereby showing that the DPPZ conjugated **C** modified AON (9) and the native counterpart (1) should be able to bind to the RNA target with equal specificity. Interestingly, DPPZ conjugated **C** modified AON also fulfils the criteria for exo/endonucleolytic stability and RNase H recruitment capability, they are also found to be non-toxic.<sup>18</sup> The summary of comparative Michaelis–Menten kinetic studies of **C** and **T** modified AONs in comparison with that of the native AON has shed light on the RNase H recruiting capability of AONs in depth in terms of substrate affinity and cleavage activity (Table 1).

#### (A) Unconjugated **C** and **T** oxetane modified AONs

The single **C** modified AON 5–RNA hybrid elicits an RNase H response in a similar manner (Table 1, Fig. 6, 7B and 8) to that of the native in both low ( $[RNA] \leq 0.01 \mu M$ ) and high ( $[RNA] \geq 1.0 \mu M$ ) RNA concentration range (Fig. 6, 7B, 8A–C, see also Figs S1–S3, S4–S14 in the supplementary information). On the other hand, the double **C** modified AON 6–RNA hybrid elicits an RNase H response that is lower at low RNA concentration,  $[RNA] \leq 0.01 \mu M$  (Figs. 7B, 8C), than the native whereas it is very comparable at high RNA concentration (Fig. 7B, 8A). This is in contrast to the behavior of **T** modified AONs (2–5) where, at high RNA concentration, **T** modified AONs have high target RNA cleavage activity by RNase H compared to the native (1) (Fig. 7A and 8A), but at low RNA concentration enzyme activity is lower than that of the native AON (Fig. 7A and 8C).

The reason for the different behavior of **T** and **C** modified AON–RNA hybrids towards RNase H tolerance at high substrate concentration could be related to the  $T_m$  of the AON–RNA duplexes. All the **T**-modified AONs were destabilized in a more pronounced manner ( $\Delta T_m \approx 6 \text{ }^\circ\text{C}$  per modification) than the **C** modified duplexes ( $\Delta T_m \approx 3 \text{ }^\circ\text{C}$  per modification) and the native. This gives a less stable enzyme–substrate complex, and obviously a less stable enzyme–product complex for the **T**-modified AONs. This means a low enzyme binding affinity of AON–RNA duplexes, which should give less  $1/K_m$ , and it is slightly less for **T**-modified AON–RNA duplexes than that for the **C** modified AONs and the native (Table 1 and Fig. 8B). Also, this means more turnover for the enzyme because of the high rate of dissociation of the enzyme–product complex, which should give more  $V_{max}$  ( $k_{cat}$ ) for **T**-modified AON–RNA duplexes than for the **C** modified AONs and the native (Table 1 and Fig. 8A).

The above explanation can be evidenced by a direct correlation between  $V_{max}$ ,  $k_{cat}$ ,  $1/K_m$  or  $V_{max}/K_m$  of RNase H with the  $T_m$  values of the corresponding **C** and **T** modified AON–RNA duplexes (Figs. 9A–C). The  $V_{max}$  for the substrates (*i.e.* duplex), containing **C** or **T** modifications, increases with the decrease in  $T_m$  of the AON–RNA duplex (Fig. 9A) which is revealed by a linear dependence of  $[\log(V_{max})]$  on  $T_m$  of AON–RNA duplexes (Fig. 9A). Conversely, the  $1/K_m$  and  $V_{max}/K_m$  values for the substrates increase with the increase in  $T_m$  of AON–RNA duplexes (Figs. 9B and C).

#### (B) DPPZ and cholesterol conjugated **C** and **T** oxetane modified AONs

The introduction of the  $\pi$  electron rich DPPZ or highly hydrophobic cholesterol residues in **C** or **T** modified AONs has different influences on the  $1/K_m$  and  $V_{max}$  or  $k_{cat}$  of RNase H (Table 1, Fig. 8A, B). DPPZ conjugation gives less binding affinity, and less or comparable catalytic activity of the RNase H compared with the native counterpart (Table 1, Fig. 8A, B). In contrast, conjugation of the hydrophobic cholesterol residue to AONs gives less binding affinity and more catalytic activity of RNase H (Table 1, Fig. 8A,B). Both DPPZ and cholesterol conjugation increase the  $T_m$  of the corresponding AON–RNA duplexes (Fig. 2), but no  $T_m$  correlation is found with the  $1/K_m$ ,

$V_{max}$  or  $V_{max}/K_m$  (Figs. 9A–C), when unconjugated AONs (1–6) are taken into consideration.

A linear dependence of  $[\log(V_{max})]$ ,  $[\log(1/K_m)]$  or  $[\log(V_{max}/K_m)]$  with the  $T_m$  of the corresponding AON–RNA heteroduplex has been also found for a short 9mer AON<sup>13</sup> and its 3'-tethered conjugates<sup>13</sup> having DPPZ or hydrophobic moieties like cholic acid, cholic acid triacetate or cholesterol residues (Fig. 10). In this group of AONs, only the DPPZ

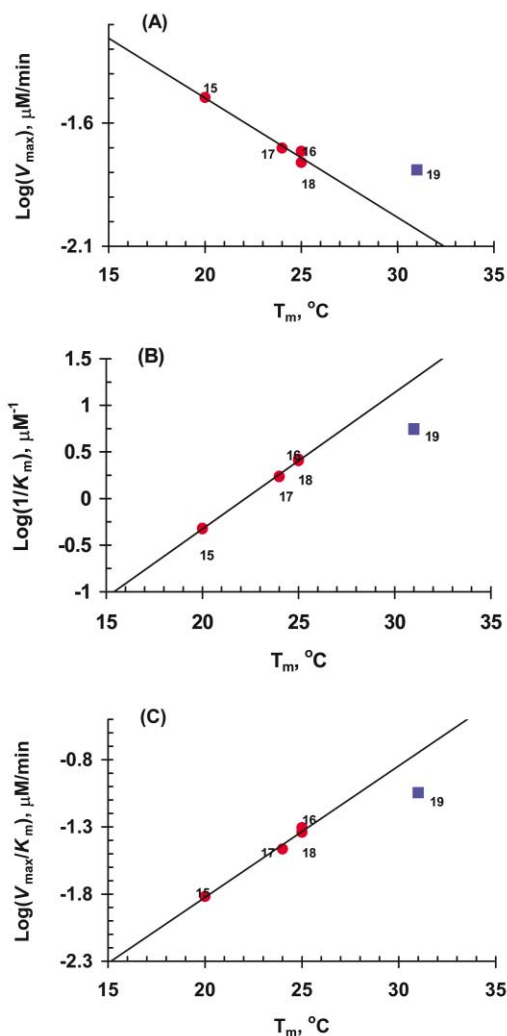


**Fig. 10** The plot of catalytic activity  $[\log(V_{max})]$  (A), binding affinity  $[\log(1/K_m)]$  (B) and effective activity  $[\log(V_{max}/K_m)]$  (C) of RNase H versus thermostability ( $T_m$ ) of the AON–RNA duplexes formed with 17mer RNA 20 and native 9mer-AON 15, Chol-AON 16, Chol(Ac)<sub>3</sub>-AON 17, Cholest-AON 18 or DPPZ-AON 19. The linear correlation was found for all AONs (15–18)–RNA 20 duplexes and exceptions for their DPPZ (■)conjugate 19. Note, the AON 19 marked with (■) is not included in the correlation equation. Correlation coefficients ( $R^2$ ) for the plots are: 0.99 for (A), 0.97 for (B) and 0.98 for (C).

moiety has an additional influence on the binding affinity, catalytic activity and effective cleavage activity of the enzyme. DPPZ conjugated 9mer AON–RNA duplex has 6 times more  $1/K_m$  and  $V_{max}/K_m$  (and less  $V_{max}$ ) because of its high  $T_m$  compared to the native, hence the plots of  $[\log(1/K_m)]$  or  $[\log(V_{max}/K_m)]$  versus  $T_m$  (Figs. 10B–C) are not linearly correlated.

The reason that 3'-tethered 9mer AONs behave so differently from the corresponding 15mer AON conjugates may be owing to the size/volume of their respective duplex in the substrate–enzyme complex, which affects recognition and interaction by the enzyme. The differences in the enzymatic behavior of the DPPZ and cholesterol tethered AONs are perhaps owing to their different chemical nature: It is likely that the DPPZ group possibly interacts with the aromatic residues of the enzyme

through  $\pi$ - $\pi$  interactions (stacking), or/and through the coordination of  $Mg^{2+}$  with the nitrogen atoms (N4 and N5) in the fused phenanthroline system of the DPPZ moiety, which can act as reservoir of this important cofactor for the cleavage reaction.<sup>15</sup> On the other hand, the poorer binding affinity of the cholesterol AON-RNA substrate to RNase H could be due to the undesirable interaction of the hydrophobic moiety with the enzyme, which can inhibit formation of the substrate-enzyme complex,<sup>16a</sup> giving poor binding affinity to the enzyme, as observed in this work.

## Conclusions

(1) Antisense oligonucleotides (AONs) with single and double oxetane **C** modifications [1',2'-oxetane cytidine [1-(1',3'-anhydro- $\beta$ -D-psicofuranosyl)cytosine] were evaluated for their antisense potentials by targeting to a 15mer complementary RNA. Although the **C** modified mixer AONs showed  $\sim 3$  °C drop per modification in melting temperature ( $T_m$ ) of their hybrid duplexes, they are found to be good substrate for RNase H, in comparison with the native AON-RNA duplex. The loss in  $T_m$  of interior **C** modified AON-RNA hybrids was regained by the introduction of non-toxic dipyrindophenazine (DPPZ) at the 3'-end (+6 °C).

(2) A detailed Michaelis-Menten kinetic analysis of RNase H cleavage showed that the single and double **C** modified AON-RNA duplexes has catalytic activity ( $k_{cat}$ ) close to that of the native. However, the enzyme binding affinity ( $1/K_m$ ) showed a slight decrease with increase in the number of modifications, which results in less effective enzyme activity ( $k_{cat}/K_m$ ) for **C** modified AON-RNA duplexes.

(3) A comparative study with the corresponding single and double 1',2'-oxetane thymidine, **T**, modified AON-RNA duplexes, where the  $T_m$  drop was  $\sim 6$  °C per modification, however, showed that the  $k_{cat}$  slightly increase and the  $1/K_m$  decrease with the increase in the number of **T** modifications, which give a lower  $k_{cat}/K_m$  also for **T** modified AON-RNA duplexes. The comparison of  $k_{cat}/K_m$  for both **C** and **T** modified AON-RNA duplexes show that RNase H activity can be achieved by the introduction of **C** without sacrificing much of the target affinity which is an inherent drawback of **T** modified AONs.

(4) All the **C** and **T** modified AON-RNA hybrids showed a correlation of  $T_m$  with  $1/K_m$ ,  $V_{max}$ , or  $V_{max}/K_m$ . The enzyme binding affinity and effective enzyme activity increase with increase of  $T_m$ ; the catalytic activity was however found to decrease with a rise in  $T_m$  of the hybrid duplexes.

(5) The **C** modified AONs, as in the **T** counterpart, showed an enhanced tolerance towards the endonuclease degradation: single **C** modification gives  $\sim 3$  fold protection and double **C** modification gives  $\sim 4$  fold protection in comparison with the native AON.

(6) Even though the enzyme catalytic activity ( $k_{cat}$ ) of DPPZ conjugated double oxetane **C** modified AON is comparable to the native, its enzyme binding affinity was two fold lower which in turn results in a the loss of  $k_{cat}/K_m$  by half. DPPZ also give enhanced protection against nucleases in human serum.

(7) 3'-Conjugation of a cholesterol moiety to the oxetane modified AONs has been found to have a less pronounced effect on RNA target affinity ( $\Delta T_m \approx +2$  to  $+3$  °C) although these conjugated AON-RNA hybrids have shown high  $k_{cat}$  of RNase H and low  $1/K_m$  and low  $k_{cat}/K_m$ , compared to the native counterpart.

(8) Thus, in this report, we show the utility of an AON having a fully phosphate backbone, by minimal (two) introduction of oxetane **C** modifications in conjunction with DPPZ, as a potential antisense candidate with no toxicity. The candidacy of oxetane modified AONs with natural phosphate backbone should be considered as an alternative, keeping in view the non-antisense activity of the phosphorothioate based AONs (see ref. 3 for a critical review).

## Materials and methods

### Materials

All solvents were dried according to the reported procedures.<sup>22</sup> The chromatographic separations were performed on Merck G60 silica gel. Thin layer chromatography (TLC) was performed on Merck pre-coated silica gel 60 F<sub>254</sub> glass backed plates and developed in following dichloromethane-methanol mixtures. System (A): 97 : 3 (v/v), (B): 95 : 5 (v/v), (C) 90 : 10 (v/v). <sup>1</sup>H-NMR spectra were recorded with Jeol GX 270 (if nothing else is indicated) and Bruker, DRX 600 spectrometers at 270 and 600 MHz, respectively, using TMS (0.0 ppm), methanol (3.4 ppm), DMSO-d<sub>6</sub> (2.6 ppm) or acetonitrile (2.0 ppm, for D<sub>2</sub>O solutions) peaks as internal standards. <sup>13</sup>C-NMR spectra were recorded with a Jeol GX 270 spectrometer at 67.9 MHz using the central peak of CDCl<sub>3</sub> (76.9 ppm), DMSO-d<sub>6</sub> (39.6 ppm) or acetonitrile (1.3 ppm, for D<sub>2</sub>O solutions) as internal standard. <sup>31</sup>P-NMR spectra were recorded with a Jeol GX 270 spectrometer at 109.4 MHz using 85% phosphoric acid as an external standard. Chemical shifts are reported in ppm ( $\delta$  scale). Thermal denaturation experiments were performed on a PC-computer interfaced Perkin Elmer UV/VIS spectrophotometer Lambda 40 with PTP-6 peltier temperature controller. Fast deprotecting phosphoramidites were purchased from Glen Research Inc. (USA). T4 polynucleotide kinase, *E. coli* RNase H (5units/ $\mu$ l) and [ $\gamma$ -<sup>32</sup>P] ATP were purchased from Amersham Biosciences (Sweden). Phosphodiesterase I (*Crotalus adamanteus* venom), DNase I (Bovine pancreas) and Human Serum (AB male) were from SIGMA

### Preparation of oxetane **C** modified building blocks

**1-(1'-O-Methanesulfonyl-6'-O-[4-toluoyl]- $\beta$ -D-psicofuranosyl)-N<sup>4</sup>-benzoylcytosine (22).** N<sup>4</sup>-Benzoylcytosine (6 g, 28 mmol) was suspended in hexamethyldisilazane (70 ml) and trimethylchlorosilane (7 ml) was added. The reaction mixture was stirred at 120 °C in nitrogen atmosphere for 16 h. The volatile material was evaporated, coevaporated with toluene and the residue was kept on an oil pump for 20 min. Sugar **21** (7.6 g, 20 mmol) was dissolved in dry acetonitrile and added to the persilylated nucleobase. The mixture was cooled to 4 °C and trimethylsilyl trifluoromethanesulfonate (4.7 ml, 26 mmol) was added dropwise under nitrogen atmosphere. After being stirred at 4 °C for 1 h, the mixture was stirred at room temperature for 18 h. Saturated NH<sub>4</sub>Cl was added to the reaction mixture and stirred for 30 minutes. The organic layer was decanted and the aqueous layer was extracted 3 times with CH<sub>2</sub>Cl<sub>2</sub>. The combined organic phase was washed first with saturated sodium bicarbonate solution and then with brine. It was then dried over MgSO<sub>4</sub>, filtered and evaporated. The resultant oil was chromatographed using 0-3% MeOH-CH<sub>2</sub>Cl<sub>2</sub> yielded an inseparable mixture of  $\alpha$  and  $\beta$  nucleosides (8 g, 15 mmol, 75%) which was coevaporated with pyridine 3 times and dissolved in 105 ml of the same solvent. The mixture was cooled in an ice bath and methanesulfonyl chloride (3.2 ml, 41.3 mmol) was added dropwise to the mixture, continued the stirring for 15 min at the same temperature. The reaction was kept in at 4 °C for 12 h, then poured into cold saturated NaHCO<sub>3</sub> solution and extracted with CH<sub>2</sub>Cl<sub>2</sub>. The organic phase was washed with brine, dried over MgSO<sub>4</sub>, filtered, evaporated and coevaporated with toluene. Chromatography of the residue using 0-3% MeOH-CH<sub>2</sub>Cl<sub>2</sub> furnished **22** (6.1 g, 9.9 mmol, 66%).  $R_f$ : 0.6 (System A).

<sup>1</sup>H-NMR (CDCl<sub>3</sub>): 8.04-7.07 (m, 11H, 4-toluoyl, benzoyl, H-5, H-6), 5.48 (d,  $J_{H-3', H-4'}$  = 5.8 Hz, 1H, H-3'), 5.16 (d,  $J_{gem}$  = 11.1, 1H, H-1'), 4.96-4.91 (m, 2H, H-4' & H-5'), 4.69 (dd,  $J_{gem}$  = 12.8 Hz,  $J_{H-5', H-6'}$  = 2.5 Hz, 1H, H-6'), 4.52 (d, 1H, H-1''); 4.3 (dd,  $J_{H-5', H-6'}$  = 3 Hz, 1H, H-6'b), 2.92 (s, 3H, CH<sub>3</sub>, OMs), 2.2 (s, 3H, CH<sub>3</sub>, 4-toluoyl), 1.64, 1.66 (s, 2  $\times$  3H, CH<sub>3</sub>, isopropyl).

<sup>13</sup>C-NMR (CDCl<sub>3</sub>): 168.2 (C=O, 4-toluoyl), 165.7 (C=O, benzoyl), 162.9 (C-4), 150.2 (C-2), 144.1 (C-6), 133.7, 133.3

(benzoyl), 129.5, 129.4, 129.1, 129, 128.8, 127.6, 125.9, (benzoyl, 4-toluoyl), 114.2 (C-5), 99.3 (C-2'), 86.5 (C-3'), 84.42 (C-5'), 81.9 (C-4'), 69.9 (C-1'), 64.7 (C-6'), 37.2 (CH<sub>3</sub>, mesyl), 25.8, 24 (CH<sub>3</sub>, isopropyl), 21.3 (CH<sub>3</sub>, 4-toluoyl).

**1-(1',3'-O-Anhydro-6'-O-[4-toluoyl]-β-D-psicofuranosyl)-N<sup>4</sup>-benzoylcytosine (23).** Compound **22** (6.1 g, 9.9 mmol) was stirred with 30 ml of 90% CF<sub>3</sub>COOH in water for 20 minute at rt. The reaction mixture was evaporated and coevaporated three times with toluene. The residue was dissolved in 40 ml of dry DMF and added dropwise to an ice cold solution of 80% NaH (510 mg, 17 mmol) in 110 ml of DMF. The mixture was stirred at room temperature overnight, quenched with 10% acetic acid solution in water and evaporated. The residue was coevaporated with xylene and made into a slurry with silica which on chromatography yielded **23** (2.3 g, 4.8 mmol, 49% after two steps). *R<sub>f</sub>*: 0.6 (System B).

<sup>1</sup>H-NMR (DMSO-d<sub>6</sub>): 8.08–7.39 (m, 11H, 4-toluoyl, benzoyl, H-5, H-6), 5.51 (d, *J*<sub>H-3', H-4'</sub> = 3.5 Hz, 1H, H-3'), 5.21 (d, *J*<sub>gem</sub> = 8.3 Hz, 1H, H-1'), 4.8–4.76 (m, *J*<sub>H-5', H-6'</sub> = 4.9 Hz, 2H, H-1'', H-6''), 4.6–4.44 (m, *J*<sub>gem</sub> = 12.4 Hz, 3H, H-4, H-5, H-6''), 2.3 (s, 3H, CH<sub>3</sub>, 4-toluoyl).

<sup>13</sup>C-NMR (DMSO-d<sub>6</sub>): 168.3 (C=O, 4-toluoyl), 166.3 (C=O, benzoyl), 164.5 (C-4), 154 (C-2), 147.2 (4-toluoyl), 144.5 (C-6), 133.7, 133.3 (benzoyl), 129.8, 129.7, 129, 128.8, 126.9 (benzoyl, 4-toluoyl), 97.7 (C-5), 92.7 (C-2'), 87.3 (C-3'), 81.1 (C-5'), 78.1 (C-1'), 70.3 (C-4'), 64 (C-6'), 21.7 (CH<sub>3</sub>, 4-toluoyl).

**1-(1',3'-O-Anhydro-β-D-psicofuranosyl)cytosine (24).** Compound **23** (2.3 g, 4.8 mmol) was dissolved in methanolic ammonia (150 ml) and stirred at room temperature for 2 days. The solvent was evaporated, the residue was dissolved in water and DCM, and the separated water phase was further washed two times with DCM, ether and subsequent evaporation of the water layer furnished **24** (1.18 g, 4.6 mmol, 96%) *R<sub>f</sub>*: 0.3 (System C).

<sup>1</sup>H-NMR (600 MHz, D<sub>2</sub>O): 7.28 (d, *J*<sub>H-5, H-6</sub> = 7.3 Hz, 1H, H-6), 5.94 (d, 1H, H-5), 5.44 (d, *J*<sub>H-3', H-4'</sub> = 3.1 Hz, 1H, H-3'), 5.14 (d, *J*<sub>gem</sub> = 8.3 Hz, 1H, H-1'), 4.76 (d, 1-H, H-1''), 4.29–4.23 (m, *J*<sub>H-4', H-5'</sub> = 8.2 Hz, *J*<sub>H-5', H-6'</sub> = 4.9 Hz, 2H, H-4' and H-5'), 3.9 (d, *J*<sub>gem</sub> = 12.3 Hz, 1H, H-6''), 3.74 (dd, 1H, H-6'').

<sup>13</sup>C-NMR (D<sub>2</sub>O): 167.2 (C-4), 157.2 (C-2), 142.8 (C-6), 97.2 (C-5), 92.4 (C-2'), 88.3 (C-3'), 83.5 (C-5'), 79.5 (C-1'), 70.4 (C-4'), 61.3 (C-6'). 1D Diff. NOE shows 6% NOE enhancement for H6-H3' and 4% NOE for H6-H1'. FAB-HRMS: [M + H]<sup>+</sup> 256.0954; calcd 256.0933. For the corresponding thymine analog (ref 12b) FAB-HRMS: [M + H]<sup>+</sup> 271.0922; calcd 271.0930.

**1-(1',3'-O-Anhydro-6'-O-dimethoxytrityl-β-D-psicofuranosyl)-N<sup>4</sup>-isobutyrylcytosine (25).** Compound **24** (1.26 g, 4.9 mmol) was coevaporated three times with dry pyridine and dissolved in the same solvent. Trimethylsilyl chloride (3.1 ml, 24.6 mmol) was added dropwise and stirred for 30 min. To the reaction mixture, isobutyryl chloride (2 ml, 19.7 mmol) was added dropwise and stirred for 3 h. The reaction was quenched by the addition of methanol (3 ml) followed by stirring for 30 min. Saturated sodium bicarbonate solution was added and then extracted 3 times with CH<sub>2</sub>Cl<sub>2</sub>. The organic phase was washed with brine and dried over MgSO<sub>4</sub> and evaporated, then coevaporated with toluene. Recrystallisation from methanol furnished the N<sup>4</sup>-isobutyryl nucleoside (1.1 g, 3.4 mmol) which was dissolved in pyridine (27 ml). 4,4'-Dimethoxytrityl chloride (1.27 g, 3.74 mmol) was added, and the mixture was stirred at room temperature overnight. Saturated NaHCO<sub>3</sub> solution was added and extracted with CH<sub>2</sub>Cl<sub>2</sub>. The organic phase was washed with brine, dried over MgSO<sub>4</sub>, filtered, evaporated and then coevaporated with toluene. The residue on column chromatography afforded **25** (2 g, 3.2 mmol, 65% in two steps). *R<sub>f</sub>*: 0.4 (System B).

<sup>1</sup>H-NMR (CDCl<sub>3</sub>): 7.51–7.15 (m, 11H, aromatic DMTr, H-6 and H-5), 6.81–6.76 (m, 4H, aromatic DMTr), 5.5 (d, *J*<sub>H-3', H-4'</sub> = 4.1 Hz, 1H, H-3'), 5.19 (d, *J*<sub>gem</sub> = 7.8 Hz, 1H, H-1'), 4.81 (d, 1H, H-1''), 4.44 (dd, *J*<sub>H-4', H-5'</sub> = 7.9 Hz, 1H, H-4'), 4.37–4.29 (m, *J*<sub>H-5', H-6'</sub> = 2.97 Hz, *J*<sub>H-5', H-6''</sub> = 5.2 Hz, 1H, H-5'), 3.77 (s, 6H, OCH<sub>3</sub>, DMTr), 3.51 (dd, *J*<sub>gem</sub> = 10.5 Hz, 1H, H-6'), 3.41 (dd, 1H, H-6''), 2.66–2.56 (m, 1H, CH, isobutyryl), 1.23, 1.21 (s, CH<sub>3</sub>, isobutyryl).

<sup>13</sup>C-NMR (CDCl<sub>3</sub>): 177.1 (C=O, isobutyryl), 163.1 (C-4), 158.4 (DMTr), 153.7 (C-2), 144.7 (C-6), 144.4, 135.8, 129.9, 128.9, 128, 127.5, 126.5, 125.1, 112.8 (DMTr), 97.5 (C-5), 92.3 (C-2'), 87.5 (C-3'), 86.5, 83.6 (C-5'), 78.8 (C-1'), 71.7 (C-4'), 62.7 (C-6'), 55.1 (DMTr), 36.5 (CH, isobutyryl), 18.9 (CH<sub>3</sub>, isobutyryl).

**1-{1',3'-O-Anhydro-4'-O-(2-cyanoethoxy(diisopropylamino)phosphino)-6'-O-(4,4'-dimethoxytrityl)-β-D-psicofuranosyl}-N<sup>4</sup>-isobutyrylcytosine (26).** To a stirred solution of **25** (1.25 g, 2 mmol) in 15 ml of CH<sub>2</sub>Cl<sub>2</sub>, 2-cyanoethoxybis(*N,N*-diisopropylamino)phosphine (0.93 ml, 2.9 mmol) was added followed by *N,N*-diisopropylammonium tetrazolide (172 mg, 1 mmol) and the stirring was maintained overnight. The reaction mixture was diluted with ethyl acetate, poured into saturated NaHCO<sub>3</sub> solution and extracted. After two additional washings with brine, organic layer was dried over MgSO<sub>4</sub>, filtered and evaporated. The residue on chromatography (30–40% EtOAc, cyclohexane + 2% Et<sub>3</sub>N) furnished **26** (1.54 g, 1.86 mmol, 93%) *R<sub>f</sub>*: 0.6 (system B) The compound was dissolved in CH<sub>2</sub>Cl<sub>2</sub> (4 ml) and precipitated from hexane at –40 °C.

<sup>31</sup>P-NMR (CDCl<sub>3</sub>): 150.74, 150.45.

**Preparation of oxetane C modified CPG solid support.** To a stirred solution of **25** (50 mg, 0.08 mmol) in 0.7 ml of CH<sub>2</sub>Cl<sub>2</sub>, succinic anhydride (16 mg, 0.16 mmol) and 4-(dimethylamino)pyridine (19.5 mg, 0.16 mmol) were added. The mixture was stirred for 4 h at rt. It was diluted with CH<sub>2</sub>Cl<sub>2</sub> and then poured into saturated NaHCO<sub>3</sub> solution. The organic phase was washed with 0.1 M citric acid (3 times), water and brine solution, dried over MgSO<sub>4</sub>, filtered and evaporated. The resulted succinate (**27**, 52 mg, 0.07 mmol) was dissolved in 6 ml acetonitrile and *N,N*-diisopropylethylamine (1.2 ml), benzotriazol-1-yloxytris(dimethylamino)phosphonium hexafluorophosphate (64 mg, 0.15 mmol), *N*-hydroxybenzotriazole (20 mg, 0.15 mmol) and 400 mg of aminopropyl CPG were added. The mixture was gently agitated for 2 h; the CPG was filtered, washed with acetonitrile, CH<sub>2</sub>Cl<sub>2</sub>, dry diethyl ether and assayed for loading (36 μmol per g of resin). The excess of amino groups on the support was then acetylated with 1 ml of acetic anhydride in 10 ml of pyridine containing 4,4-(dimethylamino)pyridine (180 mg) for 2 h. The support was then filtered and thoroughly washed with pyridine, CH<sub>2</sub>Cl<sub>2</sub> (4 times) and diethyl ether, and then vacuum dried.

#### Synthesis, deprotection and purification of oligonucleotides

All oligonucleotides were synthesized using an Applied Biosystems 392 automated DNA/RNA synthesizer. Synthesis, deprotection and purification of all oxetane **T** modified AONs,<sup>12b,c</sup> cholic acid,<sup>15</sup> cholesterol<sup>15</sup> conjugated AONs and their target RNAs were performed as previously described. For modified AONs containing oxetane **C**, fast deprotecting amidites were used, and they were deprotected by room temperature treatment of NH<sub>4</sub>OH for 16 h. All AONs were purified by reversed-phase HPLC eluting with the following systems: A (0.1 M triethylammonium acetate, 5% MeCN, pH 7) and B (0.1 M triethylammonium acetate, 50% MeCN, pH 7). The RNA target was purified by 20% 7 M urea polyacrylamide gel electrophoresis and its purity and of all AONs (greater than 95%) was confirmed by PAGE. MALDI-MS analysis: AON (**5**)

$[MH]^- = 4477.1$ ; calcd = 4474.74; AON (6)  $[MH]^- = 4503.63$ ; calcd = 4502.74; AON (9)  $[MH]^- = 5096.55$ ; calcd = 5094.74.

### UV melting experiments

Determination of the  $T_m$ s of the AON–RNA hybrids and RNA–RNA duplexes was carried out in the following buffer: 57 mM Tris-HCl (pH 7.5), 57 mM KCl, 1 mM MgCl<sub>2</sub> and 2 mM DTT. Absorbance was monitored at 260 nm in the temperature range from 3 °C to 60 °C using a Lambda 40 UV spectrophotometer equipped with a peltier temperature programmer with the heating rate of 1 °C per minute. Prior to the measurements samples (1 μM of AON and 1 μM RNA mixture) were preannealed by heating to 80 °C for 5 min followed by slow cooling till 3 °C and 30 min equilibration at this temperature.

### <sup>32</sup>P Labeling of oligonucleotides

The oligoribonucleotides, oligodeoxyribonucleotides as well as phosphorothioates were 5'-end labeled with <sup>32</sup>P using T4 polynucleotide kinase, [ $\gamma$ -<sup>32</sup>P]ATP and standard procedure<sup>23</sup>. Labeled AONs and RNA were purified by 20% denaturing PAGE and specific activities were measured using a Beckman LS 3801 counter.

### Kinetics of RNase H hydrolysis

**(A) Calibration of RNase H concentration basing on its cleavage activity.** 15mer AON 1–RNA 14 duplex:  $[AON] = 10^{-6}$  M,  $[RNA] = 10^{-7}$  M (the first control substrate)<sup>13</sup> and 15mer AON 3–RNA 14 duplex:  $[AON] = 10^{-6}$  M,  $[RNA] = 10^{-7}$  M (the second control substrate) in a buffer, containing 20 mM Tris-HCl (pH 8.0), 20 mM KCl, 10 mM MgCl<sub>2</sub>, 0.1 mM EDTA and 0.1 mM dithiothreitol (DTT) at 21 °C in 30 μl of the total reaction volume have been used as standard substrates to calibrate the amount of RNase H actually used. The percentage of RNA cleavage was monitored by gel electrophoreses as a function of time (2–5 min) (Figs. S4–S15 in the supplementary information), using of 0.06 U of RNase H, to give the initial velocity. Thus, the initial velocity of the RNase H cleavage reaction, 0.01208 μM min<sup>-1</sup> (for the first standard substrate control) or 0.01071 μM min<sup>-1</sup> (for the second standard substrate control) under the above condition corresponds to 0.06 units activity of enzyme in 30 μl of the total reaction mixture. These are based on 11 independent experiments. Since the Michaelis equation suggests that the initial velocity of the reaction linearly depends upon the enzyme concentration, therefore, using the initial velocity for the first standard substrate control or the second standard substrate control corresponding to 0.06 units per 30 μl concentration of the RNase H, two correlation coefficients were found by dividing the observed experimental initial velocity by the standard initial velocity of 0.01208 or 0.01071 μM min<sup>-1</sup>. Then, the real enzyme concentration as well as the initial velocity in each experiment was corrected using the average value of the correlation coefficients of both the standard substrate controls, which were used to calibrate the initial velocity of the RNase H promoted cleavage reaction for each substrate presented in this work.

**(B) RNA concentration dependent experiments.** <sup>32</sup>P-Labeled RNA (0.008 to 3 μM, specific activity 50 000 cpm) with AONs (5 μM) were incubated with 0.06 units of RNase H in buffer, containing 20 mM Tris-HCl (pH 8.0), 20 mM KCl, 10 mM MgCl<sub>2</sub> and 0.1 mM DTT at 21 °C. Total reaction volume was 30 μl. Prior to the addition of the enzyme reaction components were preannealed in the reaction buffer by heating at 80 °C for 5 min followed by 1.5 h equilibration at 21 °C. After 2–10 minutes, aliquots (3 μl) were mixed with stop solution (6 μl), containing 0.05 M disodium salt of the ethylenediaminetetraacetic acid (EDTA), 0.05 % (w/v) bromphenol blue and 0.05% (w/v) xylene cyanol in 95% formamide, and subjected to 20% 7 M

urea denaturing gel electrophoresis (Fig. 6, see also Figs S1–S23 in the supplementary information). The kinetic parameters  $K_m$  and  $V_{max}$  were obtained from  $v_0$  versus  $[S_0]$  plots obeying the Michaelis–Menton equation:

$$v_0 = \frac{V_{max} S_0}{K_m + S_0}$$

Values of  $K_m$  and  $V_{max}$  for this method were determined directly from  $v_0$  versus  $[S_0]$  plots by use of the correlation SigmaPlot 2000 Program, where the correlation equation was:  $y = ax/(b + x)$  where  $a = V_{max}$  and  $b = K_m$ . Since  $V_{max} = E_0 \times k_{cat}$  ( $E_0$  = initial enzyme concentration), and for all of our RNA concentration dependent kinetics, the  $E_0$  was identical, hence  $V_{max}$  is proportional to  $k_{cat}$ . In other words,  $k_{cat}$  can be understood by comparing simply the  $V_{max}$ .

### Exonuclease degradation studies

Stability of the AONs towards 3'-exonucleases was tested using snake venom phosphodiesterase from *Crotalus adamanteus*. All reactions were performed at 3 μM DNA concentration (5'-end <sup>32</sup>P labeled with specific activity 50000 cpm) in 56 mM Tris-HCl (pH 7.9) and 4.4 mM MgCl<sub>2</sub> at 22 °C. Exonuclease concentration of 17.5 ng μl<sup>-1</sup> was used for digestion of oligonucleotides. Total reaction volume was 14 μl. Aliquots were quenched by addition of the same volume of 50 mM EDTA in 95% formamide. Reaction progress was monitored by 20% 7 M urea PAGE and autoradiography.

### Endonuclease degradation studies

Stability of AONs towards endonuclease was tested using DNase 1 from bovine pancreas. Reactions were carried out at 0.9 μM DNA concentration (5'-end <sup>32</sup>P labeled with specific activity 50000 cpm) in 100mM Tris-HCl (pH 7.5) and 10 mM MgCl<sub>2</sub> at 37 °C using 30 unit of DNase 1. Total reaction volume was 22 μl. Aliquots were taken at 60, 120, 180 and 240 min and quenched with the same volume of 50 mM EDTA in 95% formamide. They were resolved in 20% polyacrylamide denaturing gel electrophoresis and visualised by autoradiography.

### Stability studies in human serum

AONs (6 μl) at 2 μM concentration (5'-end <sup>32</sup>P labeled with specific activity 90000 cpm) were incubated in 30 μl of Human Serum (male AB) at 37 °C (total reaction volume was 36 μl). Aliquots (3 μl) were taken at 5, 15, 30, 60 and 120 min, and quenched with 6 μl of solution containing 8 M urea and 50 mM EDTA, resolved in 20% polyacrylamide denaturing gel electrophoresis and visualized by autoradiography.

### Acknowledgements

Authors thank the Swedish Research Council (Vetenskapsrådet) and Philip Morris Inc (USA) for generous financial support. We also thank Dr Suresh Gohil for recording the MALDI-TOF MS. P. I. Pradeepkumar and N.V. Amirkhanov have contributed equally in this project.

### References

- (a) N. Dias and C. A. Stein, *Mol. Cancer Ther.*, 2002, **1**, 347; (b) S. T. Croke, *Methods Enzymol.*, 2000, **313**, 3; (c) S. T. Croke, *Biochem. Biophys. Acta*, 1999, **1489**, 31.
- (a) S. Kanaya, M. Ikehara *Subcell Biochemistry*, in *Proteins: Structure, Function, and Engineering*, ed. B. B. Biswas and Siddhartha Roy, Plenum Press, New York, 1995, p. 24, p. 377–422; (b) E. Zamaratski, P. I. Pradeepkumar and J. Chattopadhyaya, *J. Biochem. Biophys. Methods*, 2001, **48**, 189.

- 3 (a) C. A. Stein, *J. Clin. Invest.*, 2001, **108**, 641; (b) I. Lebedeva and C.A. Stein, *Annu. Rev. Pharmacol.*, 2001, **41**, 403–419.
- 4 M. Manoharan, *Biochem. Biophys. Acta*, 1999, **1489**, 117.
- 5 (a) S. T. Crooke, K. M. Lemonidis, L. Neilson, R. Griffey, E. A. Lesnik and B. P. Monia, *Biochem. J.*, 1995, **312**, 599; (b) W. F. Lima and S. T. Crooke, *Biochemistry*, 1997, **36**, 390.
- 6 J. Kurreck, E. Wyszko, C. Gillen and V. A. Erdmann, *Nucleic Acids Res.*, 2002, **30**, 1911.
- 7 (a) E. Uhlmann, A. Peyman, A. Rytte, A. Schmidt and E. Buddecke, *Methods Enzymol.*, 2000, **313**, 268; (b) A. Peyman, M. Helsberg, G. Kretzschmar, M. Mag, A. Rytte and E. Uhlmann, *Antiviral Res.*, 1997, **33**, 135.
- 8 (a) R. V. Giles and D. M. Tidd, *Anti-Cancer Drug Des.*, 1992, **7**, 37; (b) D. M. Tidd, *Perspect. Drug Discovery Des.*, 1996, **4**, 51.
- 9 V. K. Rait and B. R. Shaw, *Antisense Nucleic Acid Drug Dev.*, 1999, **9**, 53.
- 10 (a) K.-H. Altman, R. Kesselring, E. Francotte and G. Rihs, *Tetrahedron Lett.*, 1994, **35**, 2331; (b) M. A. Siddiqui, H. Ford, C. George and V. E. Marquez, *Nucleosides Nucleotides*, 1996, **15**, 235; (c) V. E. Marquez, M. A. Siddiqui, A. Ezzitouni, P. Russ, J. Wang, W. R. Wanger and D. M. Matteucci, *J. Med. Chem.*, 1996, **39**, 3739; (d) S. Obika, D. Nanbu, Y. Hari, K. Morio, Y. In, T. Ishida and T. Imanishi, *Tetrahedron Lett.*, 1997, **38**(50), 8735; (e) A. A. Koshkin, S. K. Singh, P. Nielson, V. K. Rajwanshi, R. Kumar, M. Meldgaard and J. Wengel, *Tetrahedron*, 1998, **54**, 3607; (f) D. G. Schultz and S. M. Grynazov, *Nucleic Acids Res.*, 1996, **24**, 2966; (g) G. Wang, J.-L. Giradet and E. Gunic, *Tetrahedron*, 1999, **55**, 7707; (h) J. Wengel, *Acc. Chem. Res.*, 1999, **32**, 301; (i) M. Sekine, O. Kurasawa, K. Shohda, K. Seio and T. Wada, *J. Org. Chem.*, 2000, **65**(12), 3571.
- 11 (a) P. Herdewijn, *Biochem. Biophys. Acta*, 1999, **1489**, 167; (b) L. Kvaerno and J. Wengel, *Chem. Commun.*, 2001, 1419–1424.
- 12 (a) P. I. Pradeepkumar, E. Zamaratski, A. Foldesi and J. Chattopadhyaya, *Tetrahedron Lett.*, 2000, **41**, 8601; (b) P. I. Pradeepkumar, E. Zamaratski, A. Foldesi and J. Chattopadhyaya, *J. Chem. Soc., Perkin Trans. 2*, 2001, 402; (c) P. I. Pradeepkumar and J. Chattopadhyaya, *J. Chem. Soc., Perkin Trans. 2*, 2001, 2074.
- 13 N. V. Amirkhanov, P. I. Pradeepkumar and J. Chattopadhyaya, *J. Chem. Soc., Perkin Trans. 2*, 2002, 976.
- 14 (a) D. Ossipov, E. Zamaratski and J. Chattopadhyaya, *Helv. Chim. Acta*, 1999, **82**, 2186; (b) E. Zamaratski, D. Ossipov, P. I. Pradeepkumar, N. V. Amirkhanov and J. Chattopadhyaya, *Tetrahedron*, 2001, **57**, 593.
- 15 N. V. Amirkhanov and J. Chattopadhyaya, *J. Chem. Soc., Perkin Trans. 2*, 2002, 271.
- 16 (a) G. Godard, A. S. Boutorin, E. Saison-Behmoaras and C. Helene, *FEBS*, 1995, **232**, 404; (b) S. T. Crooke, M. J. Graham, J. E. Zuckerman, D. Brooks, B. S. Conklin, L. L. Cummins, M. J. Greig, C. J. Guinasso, D. Kornbrust, M. Manoharan, H. M. Sasmor, T. Schleich, K. L. Tivel and R. H. Griffey, *J. Pharmacol. Exp. Ther.*, 1996, **277**, 923; (c) M. Manoharan, L. K. Johnson, C. F. Bennet, T. A. Vickers, D. J. Ecker, L. Cowsert, M. M. Frier and P. D. Cook, *Bioorg. Med. Chem. Lett.*, 1994, **4**, 1053; (d) A. S. Boutorin, L. V. Gus'kova, E. M. Ivanova, N. D. Kobetz, V. F. Zarytova, A. S. Rytte, L. V. Yurchenko and V. V. Vlassov, *FEBS Lett.*, 1989, **254**, 129; (e) A. S. Rytte, V. N. Karamyshev, M. V. Nechaeva, Z. V. Guskova, E. M. Ivanova, V. F. Zarytova and V. V. Vlassov, *FEBS Lett.*, 1992, **299**, 124.
- 17 (a) C. F. Bleczynski and C. Richert, *J. Am. Chem. Soc.*, 1999, **121**, 10889; (b) H. Gao and J. R. Dias, *Synth. Commun.*, 1997, **27**, 757; (c) W. Kramer and G. Wess, *Eur. J. Clin. Invest.*, 1996, **26**, 715; (d) T. J. Lehmann and J. W. Engels, *Bioorg. Med. Chem.*, 2001, **9**, 1827; (e) D. Opsenica, G. Pocsfalvi, Z. Juranic, B. Tinant, J. P. Declercq, D. E. Kyle, W. K. Milhous and B. A. Solaja, *J. Med. Chem.*, 2000, **43**, 3274.
- 18 Oxetane **T** and oxetane **C** modified mixmer AON with DPPZ at the 3'-end were found to be non-toxic from 1  $\mu$ M to 20  $\mu$ M in K562 Cell culture assays. A. P. Gewirtz, University of Pennsylvania, USA; personal communication.
- 19 M. Dixon, E. C. Webb, in *Enzymes*, 3rd edn., Longman Group Ltd, London, 1979, p. 60.
- 20 M. D. Sorensen, L. Kvaerno, T. Bryld, A. E. Hakansson, B. Verbeure, G. Gaubert, P. Herdewijn and J. Wengel, *J. Am. Chem. Soc.*, 2002, **124**, 2164.
- 21 C. Wahlestedt, L. Salmi, J. K. Good, T. Johnsen, T. Hokfelt, C. Broberger, F. Porreca, A. Koshkin, M. H. Jacobson and J. Wengel, *Proc. Natl. Acad. Sci. USA*, 2000, **97**, 5633.
- 22 D. D. Perrin, W. L. F. Armarego, D. R. Perrin, *Purification of Laboratory Chemicals*, 1985, Pergamon Press, Oxford.
- 23 F. M. Ausubel, R. Brent, R. E. Kingston, D. D. Moore, J. G. Seidman, J. A. Smith and K. Struhl, *Current Protocols in Molecular Biology*, 1995, 3.10.3, John Wiley & Sons, New York.